N-glycosylation of CD24 mediates cell motility but inhibits cell proliferation in colorectal cancer

Zaki Hakami[1, 2], Teresa Raposo[1], Abdullah Alsulaiman[1], William Dalleywater[1], Hassan Otifi[1,4], Charlotte Horobin[3], Karin Garrie[3], Mohammad Ilyas[1*]

[1]Division of Cancer and Stem Cells, Molecular Pathology Group, Biodiscovery Institute, School of Medicine, University of Nottingham, UK

[2]Department of Medical Laboratory Science, Faculty of Applied Medical Science, Jazan University, Jazan, Saudi Arabia

[3]School of Science and Technology, Nottingham Trent University, UK

[4]Department of Pathology, College of Medicine, King Khalid University, Abha, Saudi Arabia

*Correspondence to Prof. Mohammad Ilyas: West block A floor, Pathology Department, Queen's Medical Centre, Derby Road, NG7 2UH Nottingham, United Kingdom; mrzmi@nottingham.ac.uk, Tel+44(0)1158230735, Fax:+44(0)1158230759, Mobile:+447879437102, ORCID iD: 0000-0001-7949-7504

Highlights

- CD24 is a heavily glycosylated molecule which contains two N-glycosylation sites, and these contribute to activation of downstream targets and induction of cell motility
- Each N-glycosylation site contributes partially, and their effects appear to be additive
- The N-glycosylation sites may exert an inhibitory effect on cell proliferation
- Much of the CD24 activity is mediated through post-transcriptional effects

Abbreviated title: CD24 N-glycosylation's role in colorectal cancer

Keywords: CD24, Glycosylation, Colorectal Cancer, EMT, Metastasis

Abstract

CD24 confers features of stemness and enhances cell motility in colorectal cancer (CRC). It is heavily glycosylated and contains numerous O-glycosylation sites but just two N-glycosylation sites (N36, N52). Since N-glycosylation is thought to be important in mediating the function of glycoproteins, we hypothesized that CD24 might be dependent on N-glycosylation for its activities.

To test this hypothesis, site-directed mutagenesis was used to remove N-glycosylation sites by converting the target asparagine residues to glutamine. Each site was removed individually ($CD24^{N36Q}$ and $CD24^{N52Q}$) and in combination ($CD24^{N[36,52]Q}$), and the mutant CD24 clones were ectopically expressed in HCT116 and SW480 cells (CRC cell lines with low endogenous CD24 expression). The effect of the mutant CD24 on cell viability, cell motility and induction of downstream targets was compared to wild-type CD24 ($CD24^{WT}$) and empty vector controls (EVC).

Ectopic expression of the individually mutated clones $CD24^{N36Q}$ and $CD24^{N52Q}$ resulted in increased cell motility compared to EVC but was significantly less than that induced by $CD24^{WT}$. Ectopic expression of the double mutant clone $CD24^{N[36,52]Q}$ resulted in near-complete abrogation in the induction of cell motility. Unexpectedly, the expression of mutant clones (both single and double mutants) led to increased cell viability. Analysis of downstream targets and F-actin staining demonstrated reduced induction of known CD24 targets by the mutant vectors and a reduced cadherin-switch (a surrogate marker for Epithelial-Mesenchymal Transition (EMT).

We conclude that each N-glycosylation site contribute partially to the motility inducing activities of CD24 and that these are additive. Loss of the N-glycosylation results in an unexpected gain of proliferative function. Further studies are necessary to elucidate the exact mechanisms behind these activities.

Introduction

Colorectal cancer (CRC) is the third most common cancer globally, and it is the second most common cause of mortality [1]. Advancements in diagnosis and treatments have shown an improvement in overall survival (OS) rates for early CRC stages; however, 20% of cases present with metastasis and a further 35-45% have metastatic recurrence [2] leading to 5-year OS of <10% [3].

Tumour metastasis follows distinct steps through epithelial-mesenchymal transition (EMT) a process in which epithelial cells undergo biological changes including a loss in cell polarity, disruption of cell-cell adhesions and restructuring of the actin cytoskeleton. These changes contribute to the acquisition of invasive and migratory tendencies [4]. We have previously shown that CD24 induces cell invasion and migration in CRC, and it is therefore, a good candidate for a "metastasis-inducing" gene [5]. The invasion and migration activities are mediated through a CD24–ILK/FAK signalling pathway (unpublished data) and are accompanied by a "cadherin switch", where expression of E-cadherin is reduced and N-cadherin expression, characteristic of mesenchymal cells, is increased [6]. In multiple types of tumour, (such as breast cancer [7], gastric cancer [8], non-small cell lung cancer [8], ovarian cancer [9] and pancreatic cancer [10]) CD24 is associated with promoting cancer cell migration and invasion and with reduced OS [11, 12].

CD24 gene is located on chromosome 6q21, and it is a highly glycosylated, glycosyl-phosphatidyl-inositol-anchored (GPI) protein [13]. Human mature CD24 comprises 31 amino acids, nearly half of which are serine and threonine residues rendering it a mucin-like protein [14]. Analysis of the amino acid sequence shows that CD24 has 16 potential *O*-glycosylation sites and two potential *N*-glycosylation sites [13]. Glycosylation is a post-translational modification involving the enzymatic glycosidic linkage reaction between the anomeric hydroxyl group of sugar and a protein [15]. During the glycosylation process, carbohydrates can be attached to proteins and lipids. For *N*-glycosylation, carbohydrates are attached to an asparagine residue that appears in a specific sequon. Studies have shown that *N*-linked glycosylation's target sequence is asparagine-(X)-serine/threonine, where X can be any amino acid except for proline [16].

In normal growth and development, *O*-glycosylated residues have structural roles. In contrast, *N*-glycosylated residues have functional roles and have been shown to play a role in protein biology, including folding, secretion, stabilisation, conformation and trafficking to cellular and subcellular sites [17]. In cancer, *N*-glycosylated proteins are reported to play a role in tumour growth and development by way of enhancing the cancer cells' ability to evade immune detection, promoting uncontrolled proliferation, migration, and cell-cell adhesion [18-20].

For this study, we hypothesised that the *N*-glycosylation sites promote CD24-induced motility by regulating EMT and thereby, they may have a role in cancer metastasis. To test this, site-directed mutagenesis (SDM) was performed to mutate the two putative *N*-glycosylation sites in CD24 by substituting asparagine with glutamine. Mutant clones, including CD24 wild-type and EVC, were overexpressed in two CD24 negative CRC cell lines, HCT116 and SW480 [21]. Following cell line transfection, functional studies *in vitro* and protein/RNA analysis were performed.

Methods and Materials

Cell Culture

HCT116 and SW480 cell lines were obtained from the American Type Culture Collection (ATCC). Cells were cultured in Dulbecco's modified Eagle's medium (DMEM, GIBCO®, Invitrogen) supplemented with 10% fetal bovine serum (FBS, Sigma) and 1% L-glutamine (Sigma), incubated in a humidified 5% CO_2 environment at 37°C. The cell lines were regularly passaged every 3-4 days by dissociation with Trypsin-EDTA 0.25% (Sigma Aldrich). The cell lines were regularly subjected to monthly screening for mycoplasma infection. Identity of the cell lines was also confirmed by short-tandem repeat (STR) genotyping using PCR-single locus technology.

Site-Directed Mutagenesis (SDM)

The Asparagine to Glutamine (N-Q) point mutation was performed using a Phusion SDM kit (Thermo Fisher Scientific, CAT# F541). In this assay, the mutation was introduced at each of the *N*-glycosylation sites (i.e. N36Q and N52Q) individually in a CD24 expression construct. Briefly, the PCR mix consisted of 10µL Phusion HF buffer, 200µM dNTPs, 0.5µM each of forward and reverse primer **(Table S1)**, 1ng/µL template DNA, 0.02U/µL Phusion hot star II

DNA polymerase (2U/µL), made up to 20µL with nuclease-free water. Using the Primus 96 Thermal Cycler (MWG-Biotech Inc., Ebensburg, Germany), the cycling protocol was as follows: X1 initial denaturation cycle at 98°C for 30-sec, X25 cycles of (denaturation at 98°C for 10 sec, annealing at 67-68°C for 30 sec per primer, extension at 72°C for 3min), X1 final extension cycle at 72°C for 10min. The products were run on 1% agarose gel, and the fragments purified using a GenElute™ Gel extraction Kit (Sigma-Aldrich). The PCR products were circularised with T4 DNA ligase following the manufacturer's instructions (Thermo Fisher Scientific). 10-20ng (made up to 5 µl) of DNA plasmid was added to 10µL ligation reaction mixture (2.5 µl nuclease-free water, 2 µl rapid ligation buffer, and 0.5 µl T4 DNA ligase enzyme) and incubated at room temperature for 5min. Ligation control mixture was prepared without T4 DNA ligase. According to standard protocol, the ligated products were transformed into NEB 5α competent cells (New England BioLabs) using the heat shock method. The plasmid was extracted using a mini-prep extraction kit (Sigma-Aldrich), and the introduced mutations were confirmed by DNA sequencing.

To generate a double mutant plasmid, the same protocol was used as mentioned above. However, the constructed single mutant plasmids either N36Q or N52Q were used for SDM instead to generate a construct containing a mutation at both sites ($CD24^{N[36,52]Q}$).

Transient Transfection

The transfection protocol was as follows; 5×10^5 cells were seeded into 6-well plates containing 2mL fresh growth media and incubated for 24h. The medium was discarded, and the cells were serum-starved for 1h by adding 1.5mL Opti-MEM® reduced-serum medium (Gibco, Life Technologies) per well prior to transfection. During incubation, the transfection mixture was prepared as follows: 8µL/well of Lipofectamine™ 2000 was added to 250µL Opti-MEM® and incubated at room temperature for 5min. In a separate tube, 4µg/well of CD24 mutant plasmids or empty vector control were added to 250µL Opti-MEM®, and the two tubes were then combined and incubated for 20min at room temperature. The plasmid and Lipofectamine mixture was added to the well plates, incubated for 4-6 h. After incubation, the transfection media was replaced with 2 ml fresh growth media and the cells were harvested 24-48h post-transfection for protein extraction and *in vitro* functional assays. The transfection efficiency was determined according to the protocol provided by the Flow Cytometry Facility at the University of Nottingham **(Supplementary material).**

Protein extraction and Western Blotting

Whole-cell lysates were used for Western blotting. Protein extraction occurred following cell lysis by adding 150 µL Pierce® radioimmunoprecipitation assay (RIPA) buffer (Thermo Fisher Scientific) and 1.5 µL protease and phosphatase inhibitor cocktail (10X Thermo Fisher Scientific) in a dilution of 1:100. Protein quantification was performed using a Pierce™ BCA kit (Thermo Fisher Scientific). For Western blotting, 50µg of protein samples were added to loading buffer (one-third volume of protein sample) containing 1x NuPAGE™ sample reducing agent (10x, Thermo Fisher Scientific) denatured at 95°C. Protein fractionation occurred by running samples on a NuPAGE 4-12% Bis-Tris gel (Invitrogen) at 150V for 2h. Protein was transferred to a polyvinylidene difluoride (PVDF) membrane (Amersham, GE Healthcare Life Sciences) by using a semi-dry transfer on Bio-Rad Transblot turbo transfer system (Bio-Rad, Watford, UK). The membrane was blocked for 1hr with 5% skimmed milk (Sigma-Aldrich) in Tris-buffered saline with 0.1% Tween 20 (TBST) at room temperature, then incubated overnight at 4°C with primary antibodies: SWA11 (donated by Professor Altevogt, Germany), E-cadherin [#3195), N-cadherin [#13116], Snail [#3879], vimentin [#5741] (all from Cell Signaling Technology) and α-tubulin (Abcam, Ab7291) **(Table S2)**. The membrane was washed with TBST then incubated with appropriate horseradish peroxidase-conjugated secondary antibody (Sigma-Aldrich, Anti-mouse CAT# A4416 and Anti-Rabbit #A6154) for 1h at room temperature. The membrane was rewashed with TBST, and the visualisation occurred using enhanced chemiluminescence (ECL) detection kit (Thermo Fisher Scientific) on the Odyssey Fc imaging system (LI-COR Bioscience, UK). Protein expression was digitally calculated using the Image Studio-Lite Ver 5.2 software (LI-COR Biosciences Ltd. UK). Protein expression was normalised by calculation of the ratio between target proteins to the housekeeper α-tubulin.

RNA Extraction and Quantitative PCR

Total RNA was extracted using an RNA extraction kit (Sigma-Aldrich) according to the provided manual. 1µg to 2µg of RNA was reversed transcribed to cDNA using M-MLV reverse transcriptase following the manufacturer's protocol (**Supplementary material**). RT-qPCR was performed to determine the mRNA levels of CD24 and EMT biomarkers **(Table S3)** using GoTaq® qPCR Master Mix with SYBR green (Promega). The qPCR was performed in a total volume of 20µL per-reaction containing: 10ng of cDNA, 0.250µM each of the forward and reverse primers, 10µL of GoTaq® qPCR Master Mix and made up to 20µL with nuclease-free

water. The PCR was run on the following thermal cycles: X1 cycle hot-start activation for 2 mins at 95°C, X40 cycles (denaturation at 95°C for 15 sec, annealing at 60°C for 60 sec, extension at 72°C for 60 sec), X1 cycle melting curve stage (95°C for 60 sec, 55°C for 30 sec, 95°C for 30 sec). Relative mRNA levels of target genes in experimental conditions were normalised to porphobilinogen deaminase (PBGD, housekeeping control) and the empty vector control using Livak's comparative threshold cycle (2-ΔΔCT) method [22].

Cell Proliferation

A cell viability assay was used to quantify cell numbers. Five thousand cells were seeded into each well of 96-well plates containing 100µL growth medium and incubated 24h. The media was removed and washed twice with phosphate-buffered saline (PBS). The PrestoBlue® reagent (Invitrogen) was diluted in 10% FBS–DMEM (dilution of 1:10), and 100 µl of the mixture added to each well for 30min. Fluorescence quantification of resazurin product (resorufin) was performed using the BMG FLUOstar OPTIMA plate reader (Ortenberg, Germany; FlexStation II, Molecular Devices, San Jose, CA, USA) at 544nm excitation and 612nm emission wavelength. Post-reading, the PrestoBlue® mixture was discarded, cells were washed once with medium and then replaced with fresh growth medium, and incubated for a further 24h. Cell proliferation was evaluated at 0, 24, 48, and 72h. Relative fluorescence unit (RFU) readings were normalised to the reading obtained at 0hr and displayed relative to cell viability.

Invasion and Migration Assays

Cell migration was measured using both the transwell migration assay, and the wound healing assay whilst cell invasion was measured by transwell motility through matrigel. Assays were performed in triplicate on at least two separate occasions. Transwell migration was measured using 8.0-µm pore size Transwell polycarbonate membrane inserts (Costar, Corning). Firstly, 650µL of fresh medium (containing 10% FBS) was added to the lower receiver wells as a chemoattractant. To the upper inserts, 1×10^5 cells were seeded in 100 µl DMEM (containing 0% FBS) and incubated at 37°C in 5% CO2. Cell migration was assessed after 24h by incubation of the inserts for 5min in a new well-containing 650µL trypsin-EDTA to detach the cells. Cells were then transferred to the original well and labelled with 3µM calcein acetoxymethyl ester (Thermo Fisher Scientific) by incubation for 1hr at 37°C. Cell invasion was measured in the

same way except that before seeding, the insert was prepared by coating in 300µg/ml Matrigel (Matrigel® Matrix, Corning®) diluted in DMEM (0% FBS) and allowed to polymerise for 2h at 37°C in 5% CO_2. Visualisation of the cell motility was performed using Nikon Eclipse TiE fluorescence microscope (fluorescein isothiocyanate filter, 488nm excitation). Four random microscopic fields per well were taken at ×10 magnification, and the cells counted manually using ImageJ (National Institutes of Health, Bethesda, MD), and analysed by taking the average of the four fields per well.

Wound Healing Assays

Wound healing was assessed using Culture-Insert 2-Well 24, ibiTreat (ibidi) placed in the center of each well in 24-well plates. Following the manufacture's protocol, 1×106 cells were suspended in 1ml DMEM (0% FBS), 70µL/well was added to the insert and incubated for 24h. Following this, the inserts were removed, the cell layers were washed with PBS to remove non-adherent cells and covered by 1ml fresh medium. Wound closure was visualised at 0h and 24h using a wide-field system Okolab microscope. Cell migration across the gap was measured by calculating the surface area of the wound using ImageJ. In this assay, 10 µg/ml mitomycin C (Sigma-Aldrich) was added to inhibit cell proliferation.

F-actin staining

Filamentous actin (F-Actin) was visualised by immunofluorescence. Cells were seeded at 2×10^4cells/well in 8 well chamber slides (Corning) and incubated for 24h. They were fixed with a mixture of 4% paraformaldehyde and 5% sucrose for 10mins and permeabilised using 0.1% Triton X-100 in PBS (Sigma-Aldrich) for 5min at room temperature. Cells were stained by incubating for 1 hour with Texas Red-X phalloidin (Thermo Fisher Scientific) in 100 µl of 3% bovine serum albumin (BSA, Fisher Scientific) diluted in PBS. The nuclei were stained by incubation with 4',6-diamidino-2-phenylindole (DAPI; Sigma-Aldrich) diluted 1:10,000 in 1% BSA for 15min, and slides were mounted with Fluoroshield anti-fade mountant (Sigma-Aldrich). The slides were imaged using confocal Leica DMI4000B microscope at x20 magnification.

Statistical Analysis

Statistical analysis was performed using GraphPad Prism version 7.03 (La Jolla, CA). All data were evaluated using a two-way analysis of variance (ANOVA) to analyse cell proliferation, migration, and invasion. The mean protein expression in the western blotting was compared using the Student's *t*-test or one-way ANOVA. The value of $p<0.05$ was considered as statistically significant.

Results

Mutant constructs show overexpression of CD24.

The successful introduction of the $CD24^{N36Q}$, $CD24^{N52Q}$, and $CD24^{N[36,52]Q}$ mutations were confirmed by direct sequencing **(Fig.S2),** The mutant expression constructs, alongside expression constructs for wild-type CD24 ($CD24^{WT}$) and empty vector controls (EVC), were transfected into HCT116 and SW480 cells. Western blotting also confirmed that mutant protein from all the constructs was successfully expressed in both cell lines **(Fig.1 A, B)**. It is well known that heavily glycosylated proteins such as CD24 produce smeared bands on Western blotting and the appearance may be influenced by both the pattern and amount of glycosylation. Since we altered putative N-glycosylation sites, a change in the banding pattern would be expected in the mutant protein if they were true glycosylation sites. However, assessment of expression levels and protein size is not reliable in Western blots of glycosylated proteins. In order to ensure that the banding alterations were not due to changes in levels of the core protein, the lysates were digested using a combination of α2,3,6,8 Neuraminidase and PNGase F to remove sugar residues prior to Western blotting. A single 10kDa band was visualised in all conditions, and similar levels of both mutant and wild type proteins were shown to be expressed **(Fig. 1C, D)**.

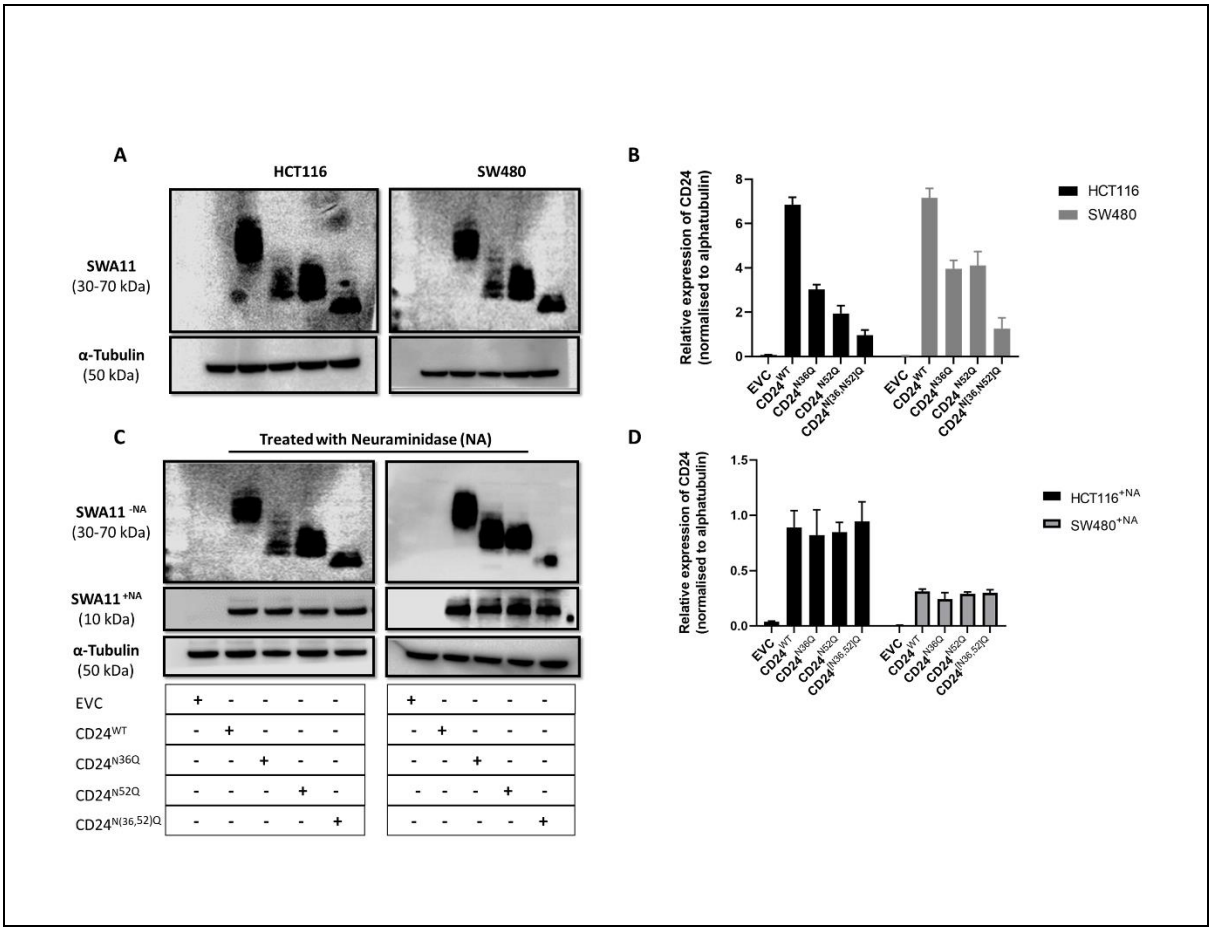

Figure 1: The expression level of CD24 shows variable glycosylation in mutant constructs.

All mutant constructs were successfully overexpressed in both HCT116 and SW480 with bands variation compared to $CD24^{WT}$ in Western blot. The cropped blots are used in the figure. The samples derive from the same experiment and that the blots were processed in parallel (A). Densitometry and quantification of western blot normalised to alpha-tubulin (B). After neuraminidase digestion, the relative protein expression of CD24 in HCT116 and SW480 cells expressing $CD24^{WT}$ and CD24 mutant constructs showed similar bands at approximately 10kDa (C). The bar graph (D) represents the quantitative densitometry analysis of western blot for CD24 protein normalised to alpha-tubulin. The figure displayed a combined result of the three experimental replicates. EVC was used as negative control and $CD24^{WT}$ as a positive control. Abbreviation: EVC; empty vector control, -NA, with Neuraminidase, +NA, without Neuraminidase.

Loss of CD24 *N*-glycosylation sites results in increased cell proliferation

Transfection efficiency can be assessed by both Western blotting and flow cytometry. Evaluation by flow cytometry showed that all mutant constructs and $CD24^{WT}$ had the same efficiency of approximately 50% to 70% **(Fig.2A, B).** Our previous studies on the effect of CD24 on cell proliferation have shown that CD24 had no role in cell proliferation [23]. In order to investigate whether the *N*-glycosylation sites of CD24 play a role in regulating cell proliferation, a PrestoBlue cell proliferation assay was used to determine proliferation at four consecutive time points **(Fig. 2 C, D)**. As expected, there was no difference in cell numbers between cells transfected with $CD24^{WT}$ and cells transfected with EVC (i.e. $CD24^{WT}$ vs EVC) in either HCT116 or SW480. However, transfection with the single-site mutant constructs $CD24^{N36Q}$ and $CD24^{N52Q}$ (i.e. $CD24^{N36Q}$ vs $CD24^{WT}$ and $CD24^{N52Q}$ vs $CD24^{WT}$) resulted in a significant increase in cell numbers from 24 hours onwards in both cell lines ($p<0.0493$ at 24h and $p<0.001$ at the other time points). The size of the effect was similar in each mutation, and no statistical difference was observed for $CD24^{N36Q}$ vs $CD24^{N52Q}$. When the cells were transfected with the double mutant construct, the cell number was significantly greater than that seen in single mutant transfections, i.e. $CD24^{N[36,52]Q}$ vs $CD24^{N36Q}$ and $CD24^{N[36,52]Q}$ vs $CD24^{N52Q}$ ($p<0.0001$ at each time point). The observations were similar in both cell lines, and the greatest effect was seen in the comparison of the double mutant with wild type, i.e. $CD24^{N[36,52]Q}$ vs $CD24^{WT}$, $p<0.0001$ at each time point for both HCT116 and SW480.

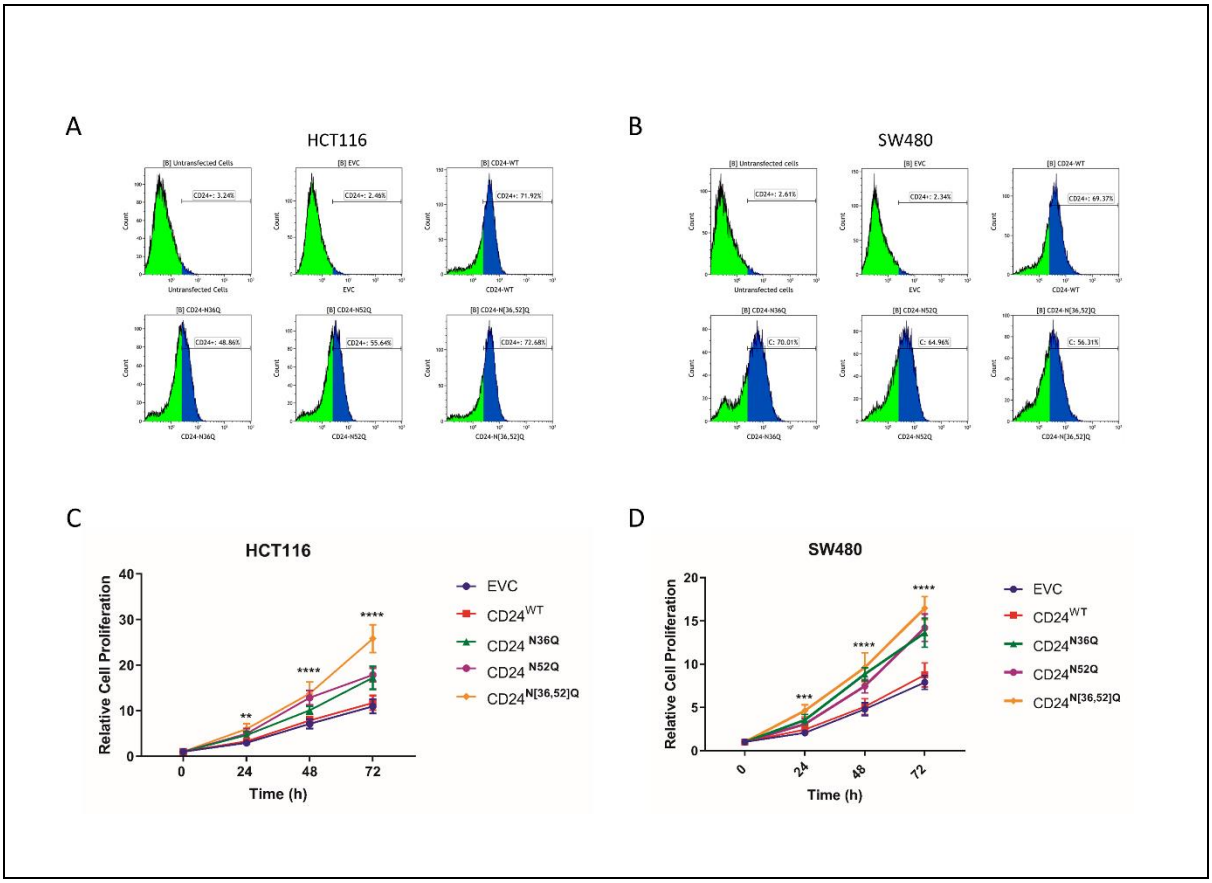

Figure 2: Mutations in the N-glycosylation sites of CD24 influences cell proliferation.

The percentage of transfection efficiency for HCT116 (A) and SW480 (B) stained with CD24+ was indicated for each construct, and the non-transfected cells and EVC were used as negative controls. The cells population that shifts to the right of the curve are CD24+ cells. Relative cell proliferation values of HCT116 (C) and SW480 (D) cell lines show a significant increase in cell viability for all mutants compared to the EVC and $CD24^{WT}$ at 24hrs (***P≤0.001), 48hrs and 72hrs (****P≤ 0.0001, respectively). Results are representative of three biological replicates, and error bars indicate the SD.

Loss of CD24 *N*-glycosylation sites results in loss of motility induction

In cell migration, we have shown that CD24 is able to induce cell motility. Examinations into the potential role of *N*-glycosylation in cell migration were performed by comparative transwell migration assays and wound healing assays using cells transfected with mutant constructs and $CD24^{WT}$. As expected, and in concordance with our previous data, $CD24^{WT}$ vs EVC demonstrated a marked increase in transwell cell migration in HCT116 and SW480 (P<0.0001 for each), **(Fig.3A)**. Transfection of the single mutant plasmids ($CD24^{N36Q}$ vs EVC

and $CD24^{N52Q}$ vs EVC) showed increased cell migration, but this was significantly less than that induced by $CD24^{WT}$ ($CD24^{N36Q}$ vs $CD24^{WT}$ and $CD24^{N52Q}$ vs $CD24^{WT}$, P= 0.0018 for HCT116, p= 0.0045 for SW480). Transfection with the double mutant $CD24^{N[36,52]Q}$ caused further reduction in cell transwell migration compared to $CD24^{WT}$ ($CD24^{N[36,52]Q}$ vs $CD24^{WT}$, P<0.0001 in both HCT116 and SW480) **(Fig.3A)**. The double mutant retained some ability to induce motility compared to the EVC in HCT116 ($CD24^{N[36,52]Q}$ vs EVC, P< 0.0114) but this appeared to be lost in SW480 (Figure 3, $CD24^{N[36,52]Q}$ vs EVC, p= NS).

Cell motility was also tested using a wound-healing assay in which residual wound size was measured over 24 hours**.** The data in **(Fig. 3C, D)** replicated those seen in the transwell migration assay in as much as the residual wound was significantly smaller in size in $CD24^{WT}$ vs EVC in both cell lines (HCT116 p<0.0001, SW480 p<0.0001). The residual wound size was significantly smaller in $CD24^{N36Q}$ vs EVC (HCT116 p> 0.0046, SW480 p<0.0072) and $CD24^{N52Q}$ vs EVC (HCT116 p<0.0002, SW480 p<0.0045) but the residual wound was significantly smaller in $CD24^{WT}$ vs $CD24^{N36Q}$ (HCT116 p<0.0242, SW480 p<0.0181 and $CD24^{WT}$ vs $CD24^{N52Q}$ (HCT116 p<0.0087, SW480 p<0.0367). Consistent with the transwell migration data, the difference in residual wound size was even more marked for $CD24^{N[36,52]Q}$ vs $CD24^{WT}$ (P<0.0001 for HCT116 and SW480, respectively) and wound healing was almost the same in $CD24^{N[36,52]Q}$ vs EVC for both HCT116 and SW480.

Our previous data showed that CD24 could also induce cell invasion through matrigel (unpublished for cell invasion). Comparative transwell invasion assays performed examinations into the potential role of N-glycosylation in cell invasion. In concordance with our previous data, $CD24^{WT}$ vs EVC demonstrated a marked increase in invasion in HCT116 and SW480 (P<0.0001 for each), **(Fig. 3B)**. As with the migration assays, single mutant plasmids showed increased cell invasion than EVC ($CD24^{N36Q}$ vs EVC and $CD24^{N52Q}$ vs EVC) in both cell lines but were less significant than $CD24^{WT}$ (P=0.0012). Double mutants $CD24^{N[36,52]Q}$ caused further reduction and near-total abrogation in invasion ($CD24^{N[36,52]Q}$ vs $CD24^{WT}$, P<0.0001 in both HCT116 and SW480. No significant difference was observed in $CD24^{N[36,52]Q}$ vs EVC for both cell lines.

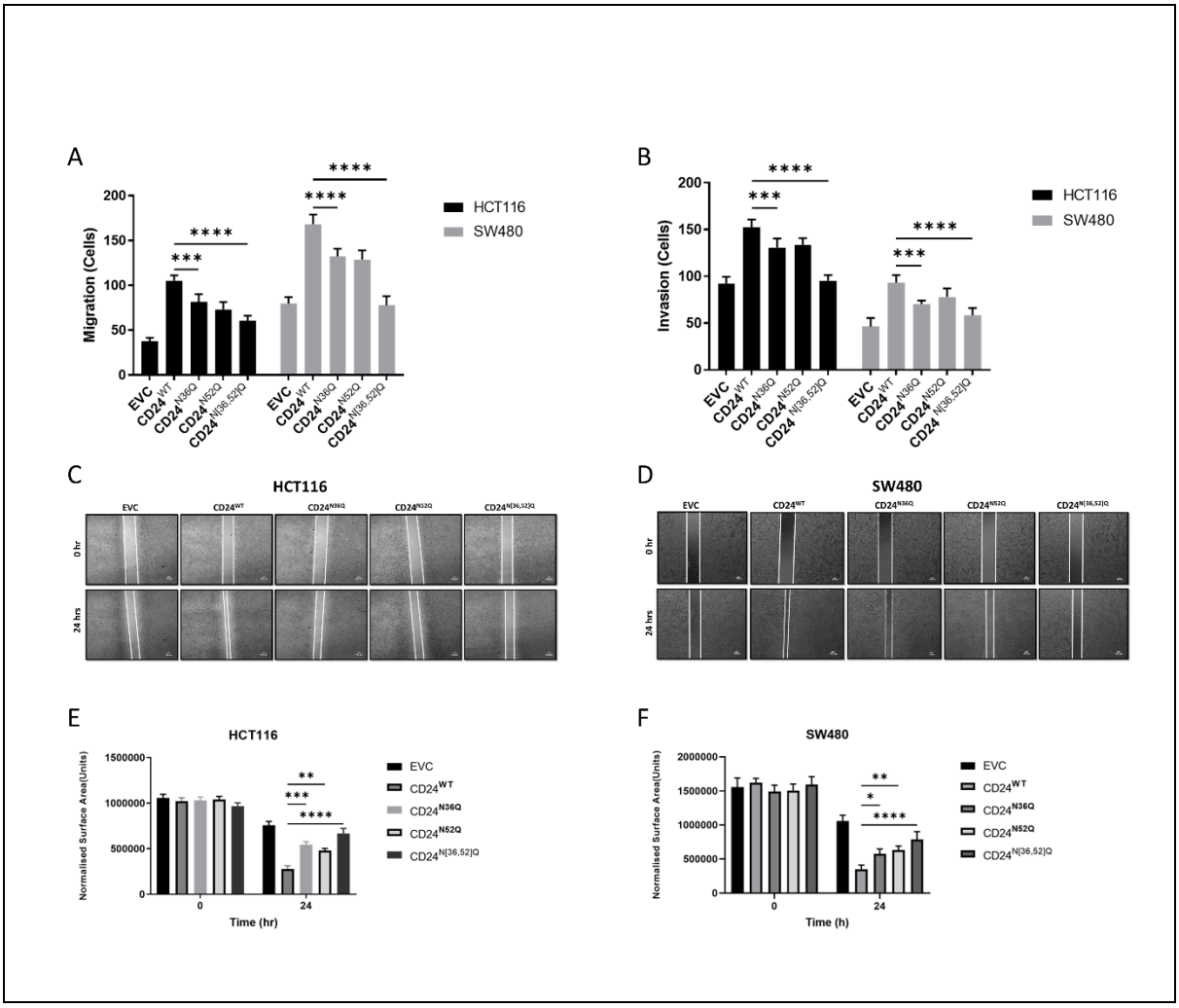

Figure 3: N-glycosylation mutation causes inhibition in CD24-induced cell invasion and migration. Transwell migration and invasion assays of HCT116 and SW460 cells transfected with $CD2^{4N36Q}$ and $CD24^{N52Q}$ shows a partial reduction compare to the control CD24 whilst assays $CD24^{N[36,52]Q}$ cells show significant depletion in both assays (A, B). Wound healing assay of HCT116 cells (C) and SW480 (D) showed that the overexpression of $CD24^{WT}$ reduces the wound gap compared to EVC. This ability was inhibited when both CD24 N-glycosylation sites are mutated. The lower panel graphs represent the normalised wound gap area of HCT116 (Left) and SW480 (Right). * $P < 0.05$, ** $P < 0.01$, *** $P < 0.001$, **** $P>0.0001$.

Loss of CD24 *N*-glycosylation sites results in loss of activation of downstream targets and reduction in epithelial-mesenchymal transition (EMT)

Previously in our lab, CD24 was shown to promote EMT [6]. To investigate the potential role of N-glycosylation on EMT, HCT116 and SW480 were transfected with $CD24^{WT}$ and $CD24^{N[36,52]Q}$, and the expression of EMT-related markers (E-cadherin, N-cadherin, Snail, and Vimentin) was measured using Western blot and qPCR. The result showed that, compared to EVC, overexpression of $CD24^{WT}$ reduces the expression of E-cadherin and increases the expression of N-cadherin in both HCT116 and SW480 **(Fig.4A, D).** This phenomenon is well described in the literature as the "cadherin switch" and is associated with EMT [24]. Conversely, transfection with $CD24^{N[36,52]Q}$ showed a complete failure to induce the cadherin switch in SW480 and a markedly diminished effect in HCT116. Complementing the cadherin switch, Snail and Vimentin levels were increased in HCT116 and SW480 by forced expression of $CD24^{WT}$. The level of these markers was lower in the forced expression of $CD24N^{[36,52]Q}$ vs $CD24^{WT}$.

We have unpublished data suggesting that CD24 may alter the target molecules' levels at both the transcriptional and post-transcriptional level. The mRNA levels of these targets were, therefore evaluated by quantitative PCR. In both cell lines, the mRNA levels of N-cadherin, Snail and Vimentin were increased by transfection with either $CD24N^{[36,52]Q}$ vs $CD24^{WT}$. There was, however, no difference in levels of mRNA expression seen between the two constructs. Similarly, no difference was seen in the levels of E-cadherin mRNA following transfection of these constructs but, in SW480, the levels of E-cadherin mRNA were higher than that in HCT116, **(Fig.4E)**.

EMT is a morphological change whereby tumour cells lose epithelial properties to gain a mesenchymal appearance**.** In order to investigate EMT further, phalloidin staining for filamentous-actin (F-actin) was performed. In comparison to cells transfected with EVC, cells transfected with $CD24^{WT}$ acquired spindle-like features, and there was increased phalloidin staining suggesting actin polymerisation. In contrast, cells overexpressing $CD24^{N[36,52]Q}$ maintained a rounded appearance with only a few cells acquiring an elongated shape. However, the staining with phalloidin was similar in $CD24^{N[36,52]Q}$ vs $CD24^{WT}$ suggesting that, despite the loss of the N-glycosylation sites, CD24 was still able to induce actin polymerisation **(Fig. 4B, C)**.

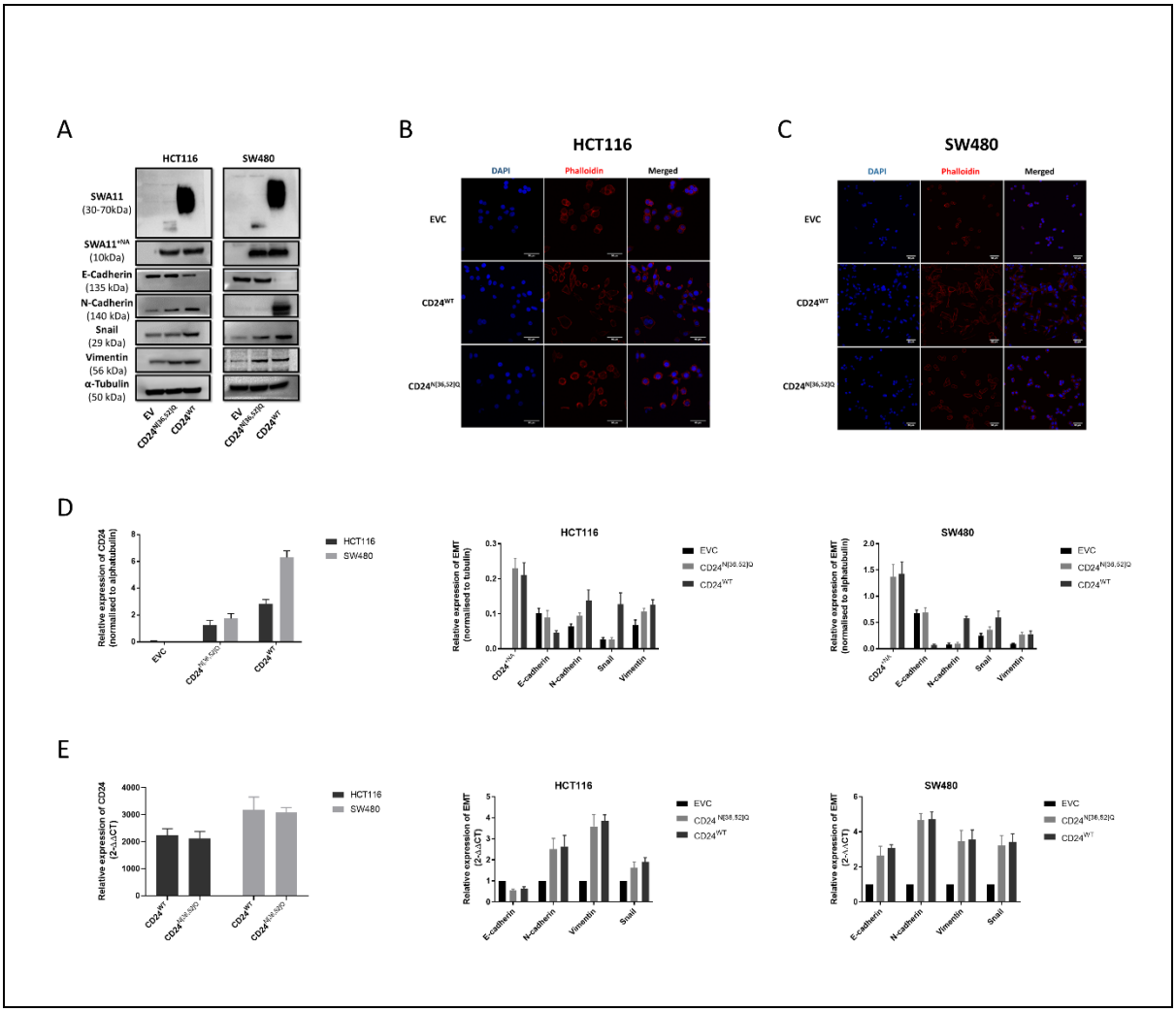

Figure 4: CD24 N-glycosylation is associated with EMT phenotype alteration and cadherin switch in CRC cells

Expression of CD24 along with EMT-related biomarkers (E-cadherin, N-cadherin, Snail, and Vimentin) was determined by WB post-transfection of HCT116 and SW480 cells with $CD24^{WT}$ and $CD24^{N[36,52]Q}$. The cropped blots are used in the figure. The membranes were cut before to exposure so that only the portion of gel containing the desired bands would be visualized. The samples derive from the same experiment and the blots were processed in parallel (A). Cytoskeleton F-actin staining at ×20 magnification shows $CD24^{WT}$ involvement in EMT morphological changes in HCT116 (B) and SW480 (C) and this restrained in $CD24^{N[36,52]Q}$. The quantitative densitometry analysis of western blot for CD24 and EMT proteins normalised to alpha-tubulin (D). RT-qPCR analysis of CD24 and EMT biomarkers in $CD24^{N[36,52]Q}$ showed no change in the mRNA levels compared to $CD24^{WT}$ overexpressed cells (E).

Discussion

CD24 is a putative oncogene expressed in various cancer types, including CRC, where its overexpression is defined as a key early event in CRC carcinogenesis [25]. Glycosylation in many proteins plays a significant role in normal biological processes and cancer development, including tumour cell proliferation, invasion, angiogenesis and metastasis [26]. Changes in a specific *N*-linked glycoprotein are associated with the development of many diseases; thus, it is crucial to identify the *N*-linked glycoproteins to facilitate disease diagnosis, prognosis, and determine treatment effectiveness [27, 28]. The structure of CD24 shows many *O*- and *N*-glycosylation sites which determine both its oncogenic properties and its role in cancer development [29].

In this study, we investigated the role of its two putative N-glycosylation sites, located around codon 36 and codon 52 in regulating cell proliferation, cell motility and EMT in two colorectal cancer cell lines. Firstly we proved that these sites were bona-fide N-glycosylation sites. At both sites, we substituted the asparagine (at codon 36 and codon 52) with the glutamine **(Fig.S2)** thereby removing the N-glycosylation target motif. This substitution would not affect the other *O*-glycosylation sites and would not create any new *O*-glycosylation sites as glutamine cannot bind to *O*-glycans [30]. Sanger sequencing confirmed that the targeted mutations had been introduced into the CD24 coding sequence. Thus, two constructs were created in which each N-glycosylation site was removed individually ($CD24^{N36Q}$ and $CD24^{N52Q}$), and a third construct in which both sites were removed ($CD24^{N[36,52]Q}$). Western blotting confirmed that each of the mutant constructs was expressing the protein, although the banding patterns were different from the protein expressed by the wild type construct ($CD24^{WT}$). The reason for the variability and reduction in the western blotting bands for the mutant constructs was initially unclear, with possible reasons including transfection artefacts, changes in protein conformation or variable glycosylation. This led us to perform neuraminidase digestion of N-glycosylation residues in all constructs, including $CD24^{WT}$. Western blotting following neuraminidase digestion showed that similar levels of full-length core protein were being expressed. The neuraminidase digestion confirmed that the variation in the banding pattern was due to loss of glycosylation rather than variation in the core protein and that the two targeted sites were indeed sites of N-glycosylation.

Previously we have shown that CD24 has no influence on proliferation in CRC cell lines [5]. Therefore, it was surprising to observe that mutation of either of the *N*-glycosylation sites resulted in increased proliferation in both HCT116 and SW480. FACS analysis had shown similar transfection efficiency for the mutant and wild-type CD24 expression constructs in both the CRC cell lines. Taken together with the Western blots showing similar levels of expression of the core protein in all mutant and wild-type constructs, we are confident that the observations were not due to variations in transfection efficiency. The size of effect was similar for each mutation but, when combined together in the construct $CD24^{N[36,52]Q}$, the effects appeared additive. There is obviously a gain-of-function acquired through the removal of the N-glycosylation sites which suggests that some signalling pathways are activated which are not activated by wild-type CD24. We would conjecture that loss of N-glycosylation may allow the CD24 to form complexes with and activate cell surface molecules (such as growth factor receptors) from which it would ordinarily be shielded by the sugar residues around codon 36 and 52. If it is a true biological phenomenon, it may be related to the role of CD24 as an inducer of stemness [19, 23]. Stem cells often have proliferative quiescence, and it is possible CD24 induces this through N-glycosylation. Alternatively, it could be an artefact of our experimental system. Either way, our data warrant further investigation to identify the targets which are leading to this observed stimulation of proliferation.

We also investigated the role of N-glycosylation in the regulation of EMT, cell migration, and cell invasion in CRC cells as these are crucial steps for tumour metastasis [31]. All assays (transwell migration and wound healing for cell migration and transwell migration through Matrigel for invasion) showed similar results, i.e. an increase in invasion and migration in both cell lines overexpressing $CD24^{WT}$ compared to EVC. Similarly, each of the individual N-glycosylation sites contributed significantly to cell motility, as seen with proliferation. The effect was additive, leading to the near-total abrogation of the ability to CD24 to induce these processes when both N-glycosylation sites were mutated. To our knowledge, this is the first time that this has been reported and our results are comparable to other studies that identify the potential role of *N*-glycosylation in inducing migratory and invasion capabilities of tumour cells [32-34]. Our data were complemented by Western blots showing that loss of the N-glycosylation sites resulted in the failure of the cadherin switch and a lower level of induction of the motility-related biomarkers Snail and Vimentin. The mRNA's evaluation showed similar

levels of induction of gene transcription of N-cadherin, Snail, and Vimentin by both the wild-type CD24 and double mutant $CD24^{N[36,52]Q}$. This would suggest that the changes observed in protein expression were mostly due to post-transcriptional modifications. The exact mechanism through which the N-glycosylation sites induce these changes is uncertain but we would conjecture that the glycosylated asparagine residues at codons 36 and 52 are able to form complexes with and activate target cell surface molecules. The additive effects could be explained by each glycosylated residue contributing a certain amount to the total avidity for the target molecules. Since both transcriptional and post-transcriptional effects are seen, it is likely that several different pathways are activated. This would fit with the multiple binding partners described for CD24 [6].

EMT is associated with the acquisition of cell motility [35]. We and others previously have demonstrated CD24 involvement in EMT of CRC cells [6, 36]. Immunofluorescence studies in line with the cell motility studies showed that cells transfected with $CD24^{WT}$ acquired a spindle-shaped mesenchymal phenotype (compared to cells transfected with EVC) and this was accompanied by actin polymerisation. In cells transfected with the double mutant, $CD24^{N[36,52]Q}$, the cells retained a rounded epithelioid phenotype similar to that seen in cells transfected with EVC. However, cells transfected with $CD24^{N[36,52]Q}$ also showed actin polymerisation at a level similar to that seen in with $CD24^{WT}$. Thus, it is apparent that CD24 can induce actin polymerisation and be mediated by mechanisms independent of N-glycosylation. It is uncertain what these mechanisms are and how they are coordinated with the N-glycosylation dependent mechanisms of motility induction.

To summarise, we have confirmed that the putative *N*-glycosylation sites of CD24 around codon 36 and codon 52 are true targets for glycosylation. For the first time, these sites have been shown to be functionally active mediators of CD24-induced EMT and cell motility (both cell migration and cell invasion) in CRC. The function of the N-glycosylation sites is mediated through both transcriptional and post-transcriptional mechanisms, although actin polymerisation may be mediated through N-glycosylation independent pathways of CD24. Unexpectedly, the N-glycosylation sites may also play a role in cell proliferation. These results suggest that CD24 *N*-glycosylation may play a role in progression and metastasis in CRC. Further studies are necessary to elucidate the mechanisms of CD24 activity in CRC and explore whether it could be a target for therapy.

Competing interests

The authors declare that they have no competing interests

Funding

Jazan University provided all financial support through the Royal Embassy of Saudi Arabia Cultural Bureau.

Authors' contributions

Z.H performed all the experimental work, the data analysis and wrote the manuscript. T.R assisted with cell culture and the analysis of the data. A.A assisted with the design of the primer sequences. W.D assisted with the design of the primer sequences and revised the manuscript. H.O assisted in result interpretation. C.H and K.G edited and reviewed the manuscript. M.I designed the study and edited and revised the manuscript. All authors read and approved the final version of the manuscript.

Acknowledgements

The author would like to express the deepest appreciation to all colleagues in the Pathology Research Group and the Division of Cancer and Stem cells for their kind support and assistance.

References

1. Bray F, Ferlay J, Soerjomataram I, Siegel RL, Torre LA, Jemal A. Global cancer statistics 2018: GLOBOCAN estimates of incidence and mortality worldwide for 36 cancers in 185 countries. CA: a cancer journal for clinicians. 2018;68(6):394-424.
2. Tauriello DVF, Calon A, Lonardo E, Batlle E. Determinants of metastatic competency in colorectal cancer. Molecular oncology. 2017;11(1):97-119.
3. Brenner H, Kloor M, Pox CP. Colorectal cancer. Lancet (London, England). 2014;383(9927):1490-502.
4. Pearson GW. Control of Invasion by Epithelial-to-Mesenchymal Transition Programs during Metastasis. J Clin Med. 2019;8(5).
5. Ahmed MA, Jackson D, Seth R, Robins A, Lobo DN, Tomlinson IP, et al. CD24 is upregulated in inflammatory bowel disease and stimulates cell motility and colony formation. Inflammatory bowel diseases. 2009;16(5):795-803.
6. Hasan Ahmed MA, Ilyas M. CD24 expression is associated with epithelial mesenchymal transition (EMT) phenotype and alterations in actin cytoskeleton in colorectal cancer. Pathology. 2014;46:S105.
7. Rostoker R, Abelson S, Genkin I, Ben-Shmuel S, Sachidanandam R, Scheinman EJ, et al. CD24+ cells fuel rapid tumor growth and display high metastatic capacity. Breast Cancer Research. 2015;17(1):78.

8. Kristiansen G, Schlüns K, Yongwei Y, Denkert C, Dietel M, Petersen I. CD24 is an independent prognostic marker of survival in nonsmall cell lung cancer patients. British Journal of Cancer. 2003;88(2):231-6.
9. Huang L, Lv W, Zhao X. CD24 as a Molecular Marker in Ovarian Cancer: A Literature Review. Cancer Translational Medicine. 2016;2(1):29-32.
10. Salaria S, Means A, Revetta F, Idrees K, Liu E, Shi C. Expression of CD24, a Stem Cell Marker, in Pancreatic and Small Intestinal Neuroendocrine Tumors. American journal of clinical pathology. 2015;144(4):642-8.
11. Baumann P, Cremers N, Kroese F, Orend G, Chiquet-Ehrismann R, Uede T, et al. CD24 expression causes the acquisition of multiple cellular properties associated with tumor growth and metastasis. Cancer Res. 2005;65(23):10783-93.
12. Lee KM, Ju JH, Jang K, Yang W, Yi JY, Noh DY, et al. CD24 regulates cell proliferation and transforming growth factor beta-induced epithelial to mesenchymal transition through modulation of integrin beta1 stability. Cellular signalling. 2012;24(11):2132-42.
13. Motari E, Zheng X, Su X, Liu Y, Kvaratskhelia M, Freitas M, et al. Analysis of Recombinant CD24 Glycans by MALDI-TOF-MS Reveals Prevalence of Sialyl-T Antigen. Am J Biomed Sci. 2009;1(1):1-11.
14. Kay R, Rosten PM, Humphries RK. CD24, a signal transducer modulating B cell activation responses, is a very short peptide with a glycosyl phosphatidylinositol membrane anchor. J Immunol. 1991;147(4):1412-6.
15. Protein Glycosylation, an Overview. eLS.
16. Aebi M. N-linked protein glycosylation in the ER. Biochimica et biophysica acta. 2013;1833(11):2430-7.
17. Spiro RG. Protein glycosylation: nature, distribution, enzymatic formation, and disease implications of glycopeptide bonds. Glycobiology. 2002;12(4):43R-56R.
18. Reily C, Stewart TJ, Renfrow MB, Novak J. Glycosylation in health and disease. Nature Reviews Nephrology. 2019;15(6):346-66.
19. Kim S-K, Park J-A, Zhang D, Cho S-H, Yi H, Cho S-M, et al. Sustainability of CD24 expression, cell proliferation and migration, cisplatin-resistance, and caspase-3 expression during mesenchymal-epithelial transition induced by the removal of TGF-β1 in A549 lung cancer cells. Oncology letters. 2017;14(2):2410-6.
20. Sriram V, Willard CA, Liu J, Brutkiewicz RR. Importance of N-linked glycosylation in the functional expression of murine CD1d1. Immunology. 2008;123(2):272-81.
21. Schneider M, Huber J, Hadaschik B, Siegers GM, Fiebig H-H, Schüler J. Characterization of colon cancer cells: a functional approach characterizing CD133 as a potential stem cell marker. BMC Cancer. 2012;12(1):96.
22. Livak KJ, Schmittgen TD. Analysis of Relative Gene Expression Data Using Real-Time Quantitative PCR and the 2−ΔΔCT Method. Methods. 2001;25(4):402-8.
23. Ahmed MA, Jackson D, Seth R, Robins A, Lobo DN, Tomlinson IP, et al. CD24 is upregulated in inflammatory bowel disease and stimulates cell motility and colony formation. Inflamm Bowel Dis. 2010;16(5):795-803.
24. Maeda M, Johnson KR, Wheelock MJ. Cadherin switching: essential for behavioral but not morphological changes during an epithelium-to-mesenchyme transition. Journal of Cell Science. 2005;118(5):873-87.
25. Sagiv E, Memeo L, Karin A, Kazanov D, Jacob–Hirsch J, Mansukhani M, et al. CD24 Is a New Oncogene, Early at the Multistep Process of Colorectal Cancer Carcinogenesis. Gastroenterology. 2006;131(2):630-9.
26. Barkeer S, Chugh S, Batra SK, Ponnusamy MP. Glycosylation of Cancer Stem Cells: Function in Stemness, Tumorigenesis, and Metastasis. Neoplasia. 2018;20(8):813-25.
27. Drake RR. Glycosylation and cancer: moving glycomics to the forefront. Advances in cancer research. 2015;126:1-10.

28. Schwarz F, Aebi M. Mechanisms and principles of N-linked protein glycosylation. Current opinion in structural biology. 2011;21(5):576-82.
29. Rodrigues JG, Balmaña M, Macedo JA, Poças J, Fernandes Â, de-Freitas-Junior JCM, et al. Glycosylation in cancer: Selected roles in tumour progression, immune modulation and metastasis. Cellular immunology. 2018;333:46-57.
30. Bause E, Legler G. The role of the hydroxy amino acid in the triplet sequence Asn-Xaa-Thr(Ser) for the N-glycosylation step during glycoprotein biosynthesis. The Biochemical journal. 1981;195(3):639-44.
31. van Zijl F, Krupitza G, Mikulits W. Initial steps of metastasis: cell invasion and endothelial transmigration. Mutation research. 2011;728(1-2):23-34.
32. Aigner S, Ramos CL, Hafezi-moghadam A, Lawrence MB, Friederichs J, Altevogt P, et al. CD24 mediates rolling of breast carcinoma cells on P-selectin. The FASEB Journal. 1998;12(12):1241-51.
33. Overdevest JB, Thomas S, Kristiansen G, Hansel DE, Smith SC, Theodorescu D. CD24 Offers a Therapeutic Target for Control of Bladder Cancer Metastasis Based on a Requirement for Lung Colonization. Cancer Research. 2011;71(11):3802.
34. Li L, Chen J, Ge C, Zhao F, Chen T, Tian H, et al. CD24 isoform a promotes cell proliferation, migration and invasion and is downregulated by EGR1 in hepatocellular carcinoma. Onco Targets Ther. 2019;12:1705-16.
35. Mittal V. Epithelial Mesenchymal Transition in Tumor Metastasis. Annual review of pathology. 2018;13:395-412.
36. Okano M, Konno M, Kano Y, Kim H, Kawamoto K, Ohkuma M, et al. Human colorectal CD24+ cancer stem cells are susceptible to epithelial-mesenchymal transition. Int J Oncol. 2014;45(2):575-80.

Supplementary Material:

Supplementary tables:

Supplementary Table 1: Primer sequences used for site-directed mutagenesis (SDM)

SDM-Primers	Forward Phospho (5' ->3')	Reverse Phospho (5' ->3')
CD24^{N36Q}	GGAACTTCAAGTCAATCCTCCCAGAGT	AGTTGTTGTTTCACTGGAATAAATCTGCG
CD24^{N52Q}	CCAAATCCAACTCAAGCCACCACCAAG	GGCCAACCCAGAGTTGGAAGTACTC

Supplementary Table 2: Details of relevant primary and secondary antibodies used for Western blot

Antibody	Provider	Species	Diluent	Ab_1 dilution	Ab_2 dilution
CD24 (SWA11)	Prof. Altevogt P (DKFZ, Heidelberg)	Mouse	5% Skimmed Milk+0.1% Tween PBS	1:1000	1:5000
E-cadherin	Cell signalling	Rabbit	5% BSA+0.1% Tween TBS	1:1000	1:5000
N-cadherin	Cell signalling	Rabbit	5% BSA+0.1% Tween TBS	1:1000	1:5000
Snail	Cell signalling	Rabbit	5% BSA+0.1% Tween TBS	1:000	1:5000
Vimentin	Cell signalling	Rabbit	5% BSA+0.1% Tween TBS	1:000	1:5000
Tubulin	Abcam	Mouse	5% Skimmed Milk+0.1% Tween PBS	1:000	1:5000

Supplementary Table 3: Primer sequences used for quantitative real-time PCR

Gene	Forward primer (5' ->3')	Reverse primer (5' ->3')
CD24	GCTCCTACCCACGCAGATTTA	TGGTGGTGGCATTAGTTGGA
CTEN	CCTTCGTGTGCCAGCATTCC	GCACCTCCCAGTTCTCTCTGTG
E-cadherin	CGTCCTGGGCAGAGTGAAT	TTTGAATCGGGTGTCGAGGG
N-cadherin	AGGCTTCTGGTGAAATCGCA	TGCAGTTGCTAAACTTCACATTG
Vimentin	CGGGAGAAATTGCAGGAGGA	AAGGTCAAGACGTGCCAGAG
Snail 1	AATCCAGAGTTTACCTTCCAGCA	TCCCAGATGAGCATTGGCAG
PBGD (Reference)	GGAGCCATGTCTGGTAACGG	CCACGCGAATCACTCTCATCT

Supplementary Figures

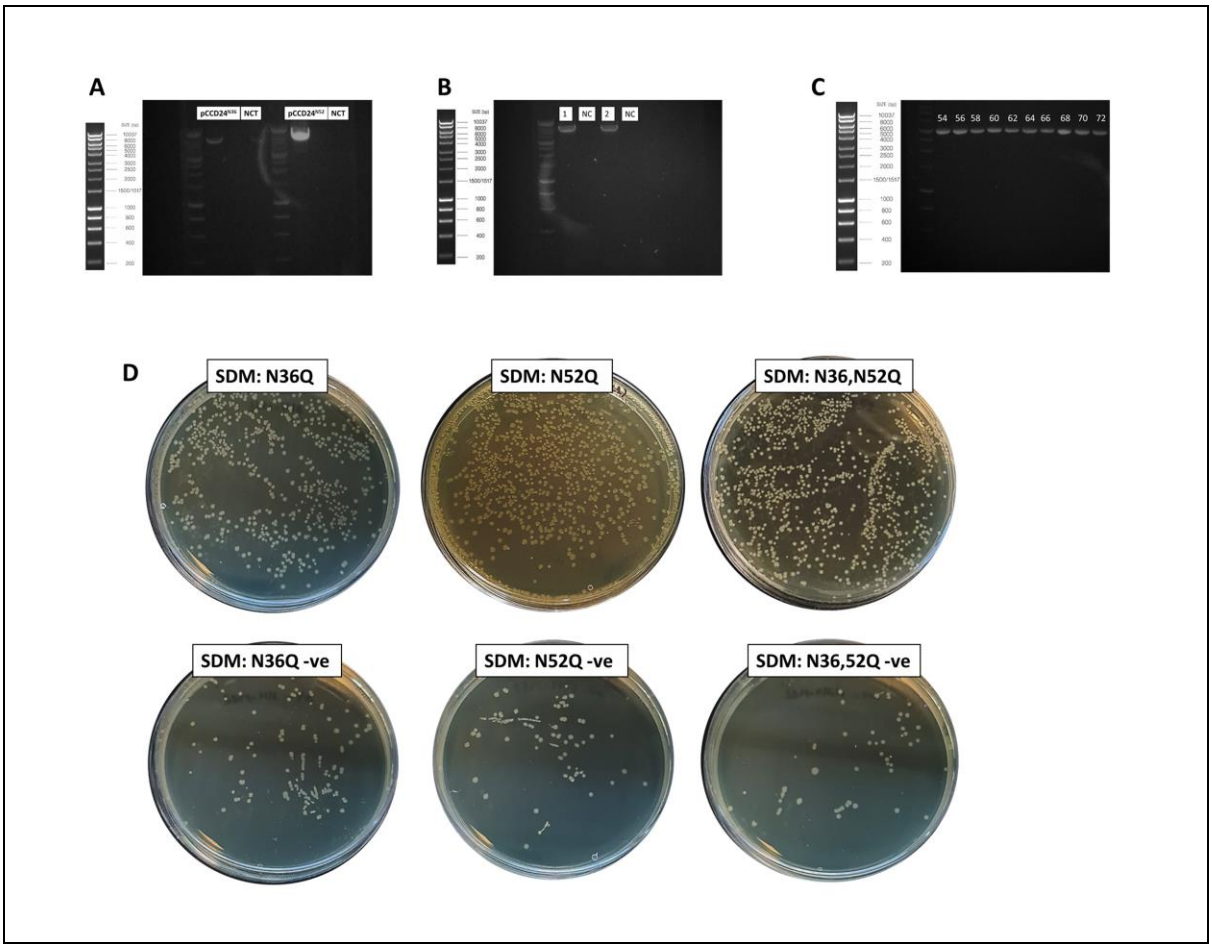

Supplementary Figure 1: Determination of SDM confirmation in $CD24^{N36Q}$, $CD24^{N52Q}$, and $CD24^{N[36,52]Q}$ Plasmids with Gel Electrophoresis and Colony Formation.

Gel electrophoresis of the SDM products produced bright bands at the correct molecular size. **(A, B)** Primers were amplified at 68°C. No band was observed in the no-template control lane. **(C)** Site-directed mutagenesis was performed on two sets of back to back primers—a gradient PCR for optimising the annealing temperature designed primers. Showing the correct molecular weight of 5747kb. **(D)** Bacterial colony formation in mutant clones ($CD24^{N36Q}$, $CD24^{N52Q}$, and $CD24^{N[36,52]Q}$) compared to the negative control, showing successful ligation. All experiments performed in triplicate.

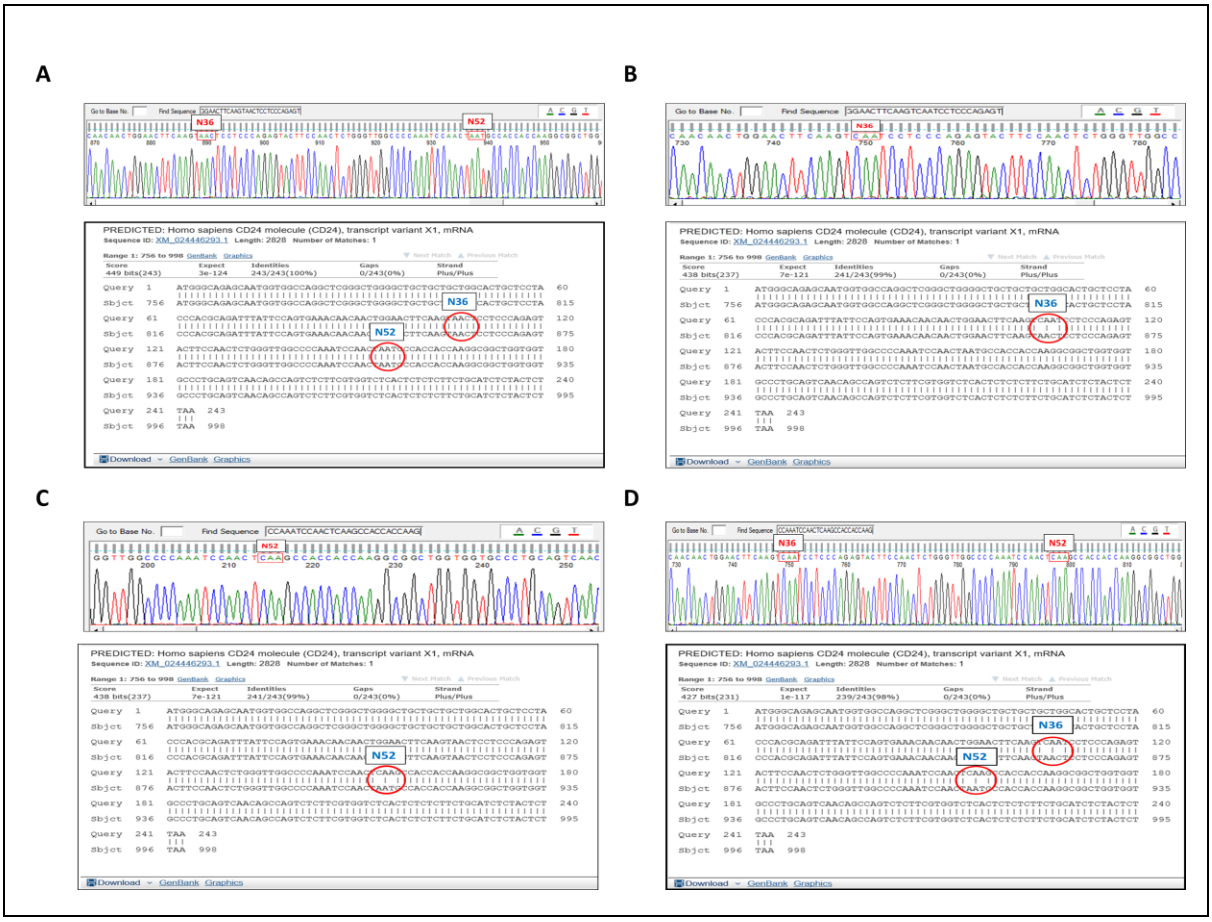

Supplementary Figure 2: Gene sequencing analysis using Finch software and alignment tool (Bast2). The presence of the CD24 gene without any mutation at both indicated codons N36 and N52 with 100% of nucleotides homology (highlighted) **(A)**. The single-mutant clones showed the desired mutation at N36, i.e. AAC to CAA **(B)**, and N52, i.e. AAT to CAA **(C)** with 99% homology in nucleotides sequence (top). The double-mutant clone showing the mutation at both N36 and 52 simultaneously, and the alignment tool showed 98% similarity in nucleotides sequence) **(D)**.

Supplementary methods:

Flow cytometry:

Transfection efficiency for cells overexpressed with $CD24^{WT}$ and mutant clones was determined using FACS analysis. Twenty four hours post-transfection, the cells were detached using Trypsin-EDTA and resuspended in sterile-filtered PBA (Phosphate buffered saline +1% bovine serum albumin). The cell suspension washed twice using PBA buffer by centrifugation for 5min at 300g. The cell was counted using an automated cell counter, and the volume of cells in PBA was adjusted at $2x10^6$/ml and pelleted by centrifugation at 300g for 5 min. Then the cell pellet resuspended in 100µl of PBA and incubated with CD24 (SWA11) antibody (1:100) for 60 min on ice. The antibody was washed twice by adding 1ml of PBA and centrifuged for 5 min at 300g. The cell pellet resuspended in 100µl of PBA and Alexa Fluor 488 goat anti-mouse conjugated secondary antibody (Invitrogen) was added. The cells were incubated for 30min on ice in the dark and then washed twice with PBA. The supernatant was removed, the pellet was vortexed and resuspended with 500µl of 4% formaldehyde. The transfection efficien cy was assessed by determining the ratio of cells overexpressing CD24 using a Beckman Coulter FC500 Flow Cytometer (Beckman Coulter) located in the Flow Cytometry Facility at Medical School, Queen Medical Centre. The data were analysed using Kaluza analysis 2.1 software (Beckman coulter Inc.), in which the cells were gated for identification of the CD24+ population using non-transfected cells as a control.

Complementary DNA (cDNA) synthesis:

The cDNA was synthesised from RNA templates as follows: 15µL reverse transcription master mix per reaction was prepared by adding 0.5µg random hexamers (Thermo Fisher Scientific) to 1-2µg RNA, and nuclease-free water, incubated for 5mins at 70°C, then by 5mins at 4°C. Followed by making 10µL/ reaction of the bulk mixture containing: 5µL M-MLV-RT buffer (5X Promega), 1.25µL dNTPs (10mM, Promega), 1µL M-MLV-RT enzyme (Promega), 25U RNase inhibitor (0.625µL) (Promega), made up to 10µL with distilled water. 10µL of the bulk mixture was added to the 15µl M-MLV template: hexamer mix to a total volume of 25µl and incubated for 1hr at 37°C, then 10mins at 95°C.